Nanogratings containing sub-10-nm wide trenches by dimension reduction from sloped polymer profile

Krutarth Trivedi and Walter Hu[a)]
Department of Electrical Engineering, University of Texas at Dallas, Richardson, Texas 75080

(Received 1 July 2009; accepted 26 October 2009; published 3 December 2009)

Large area nanograting patterns are useful in many applications but difficult to fabricate. The authors demonstrate a low temperature dimension reduction method, as a cost-effective alternative to high resolution lithography, to define nanogratings as narrow as 8–10 nm. In this process, the slope of prepatterned polymer gratings, with pitch of 200 nm or larger and width of 100 nm or larger, is contrillably changed from the original straight to curved or sloped. Then, shadow metal evaporation is used to coat the sloped polymer profile to define a much narrower opening. This opening is then transferred to underlying material by plasma etching to form sub-10-nm trenches. The width of trenches can be well controlled by both slope of the profile and angle of metal evaporation. Low processing temperature (as low as 55–85 °C—depending on polymer) allows this method to be used with a wide variety of materials. © *2009 American Vacuum Society.*
[DOI: 10.1116/1.3264683]

I. INTRODUCTION

Nanograting patterns are the building blocks of many devices used in a variety of applications, e.g., nanofluidics,[1] optoelectronics,[2] nanowire sensors,[3] solar cells,[4] tissue engineering,[5] etc. Nanogratings are typically defined by scanning beam lithography or advanced photolithography,[6,7] followed by an etching or lift-off process to transfer patterns from resist to substrate. As dimensions are controlled by dose in electron-beam (e-beam) and photolithography, it is challenging to produce ultrasmall nanoscale patterns over large areas consistently. More importantly, the sequential nature of e-beam lithography or the high cost of advanced photolithography makes writing large areas of continuous nanogratings prohibitively time consuming and/or expensive. Nanoimprint lithography is often used as a cost-effective process to produce nanostructures over large areas.[8] However, fabrication of imprint molds, particularly for ultrafine features, still demands conventional high resolution lithography.

Reducing the size of larger patterns is one low-cost strategy to define ultrasmall patterns without the use of high resolution lithography. One widely used scheme to reduce dimensions of silicon gratings is oxidation. Several novel, yet unconventional methods such as edge lithography,[9] size reduction lithography,[10] and nanopattern oxidation[11] utilize various forms of this technique to reduce dimensions during or after the pattern transfer step. However, these techniques are limited by the high temperatures required for silicon oxidation, surface and edge variations, and oxidation nonuniformities resulting in high line edge roughness (LER).[11,12] Moreover, oxidation based techniques are not applicable to materials other than silicon, e.g., III-V compound semiconductors or even organic materials. Recently, a set of techniques called self-perfection by liquefaction, or SPEL, has shown promising capability to reduce dimensions by melting and reflowing nanoimprinted polymer structures.[13,14] Polymer reflow may cause difficulty in controlling uniformity over large areas for dimensions down to the sub-10-nm regime. Another method to reduce grating dimension is SAFIER, a temperature dependent (as high as 160 °C) shrinking process in which several coat and bake cycles with a specialized coating material produce linewidths of as low as ~20 nm.[15] Shadowed or oblique angle metal evaporation has long been used to fabricate small gaps in materials.[16,17] Its reliability largely depends on the geometry of structures onto which the metal is evaporated.

In this work, we develop a simple dimension reduction method to fabricate gratings with trenches as narrow as sub-10-nm. Dimension reduction is achieved by controlling the shape and slope of polymer grating sidewalls, facilitating smooth and directed selective metal coating by oblique angle evaporation, which effectively reduces pattern dimension. Plasma etching is used to transfer the reduced gratings to substrate materials. This low temperature process can be applied to a wide variety of materials without the need for high resolution lithography.

II. PROCESS AND RESULTS

Initial grating patterns are defined in resist on top of a substrate, either by photolithography or nanoimprint lithography. Resist is chosen based on patterning method, as certain resists prefer either nanoimprint or photolithography. Patterns in each resist can be calibrated to yield the desired profile shapes; in our case, we have demonstrated control of profile shape with poly(methyl methacrylate) (PMMA) and SU-8 for gratings defined by nanoimprint lithography as well as S1813 for photolithographically defined gratings. As our dimension reduction method is applicable to all substrates, the choice of substrate is inconsequential; in our case, we use oxidized silicon, as SiO_2 has sufficiently high selectivity to silicon during plasma etching.

[a)]Electronic mail: walter.hu@utdallas.edu

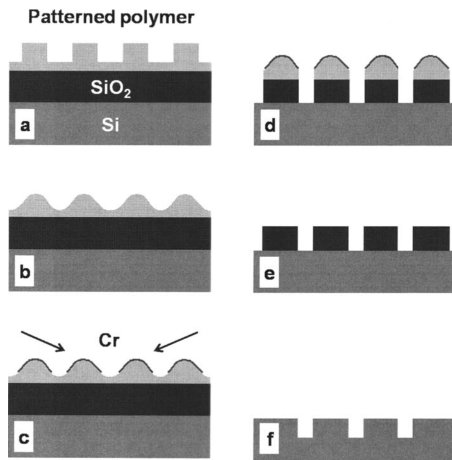

FIG. 1. Process flow for dimension reduction. (a) Spin coated polymer is imprinted with a mold containing a 100 nm line and space grating pattern. (b) The pattern is heated to produce sloped sidewalls. (c) Cr is evaporated at an oblique angle, leaving small gaps in-between. (d) The exposed polymer residue is etched with oxygen plasma, followed by oxide etch in fluorine plasma. (e) The remaining Cr and polymer are removed by wet etching. (f) The patterns may optionally be transferred to Si and the SiO_2 mask may be removed by wet etching.

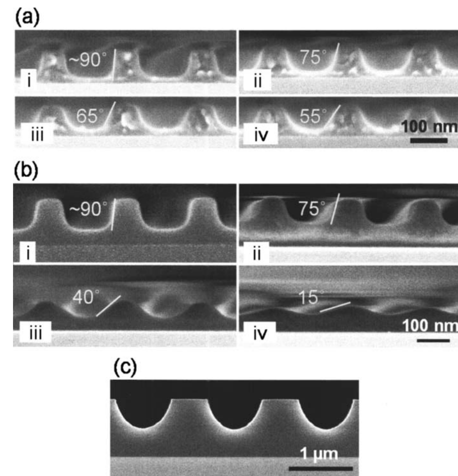

FIG. 2. Cross sectional SEM images of (a) a nanoimprinted PMMA grating (i) before heating, (ii) after heating at 125 °C for 30 s, (iii) 1 min, and (iv) 2 min. (b) A nanoimprinted and cross-linked SU-8 grating (i) before heating, (ii) after heating at 55 °C for 15 s, (iii) 1 min, and (iv) 2 min. (c) A S1813 grating defined by photolithography, exposed at a dose of 50 mJ/cm^2.

The process flow is shown in Fig. 1. Polymer gratings of larger size (100 nm or larger) are first patterned and their profile is controllably altered to have curvature or slope. Metal is selectively coated onto sloped sidewalls of grating patterns via shadow evaporation, producing small openings in between the metal. Next, the patterns with reduced openings are transferred by plasma etching into the underlying substrate. In the case of nanoimprinted gratings, PMMA and SU-8 were imprinted with a 100 nm line and space grating mold (Nanonex). The mold was treated with perfluorodecyltrichlorosilane to prevent adhesion of polymer to the mold during demolding. PMMA was imprinted at 175 °C for 15 min with a pressure of 60 bars. SU-8 was imprinted at 85 °C for 15 min with a pressure of 30 bars. For microscale gratings, photolithography was used to make ~1 μm line and space grating in S1813 (Shipley).

A sloped profile of polymer lines is crucial, as it facilitates uniform shadowed metal coating on the patterned polymer. Without a sloped profile, the metal coating is not directed by the underlying polymer, resulting in loss of control over final trench dimension and significant LER in transferred patterns. In the case of nanoimprinted patterns, a sloped and almost sinusoidal profile was achieved by controlled melting or relaxation of the imprinted polymer grating directly after demolding. The slight melting or relaxation of polymer grating would likely reduce the surface roughness, as indicated by SPEL.[13,14] As shown in Figs. 2(a) and 2(b), both the temperature and time can significantly affect the shape of the patterned polymer gratings, with higher temperature and longer time resulting in decreasing sidewall slope. To minimize the time, temperature was calibrated so that the profile shape would change significantly in a matter of seconds or minutes, as shown in Fig. 3(a). PMMA (T_g ~ 100 °C) required a significantly higher temperature of 125 °C compared to 55 °C for SU-8 (T_g ~ 55 °C) to produce similarly sloped sidewalls; this difference could be attributed to differences in molecular weight, as the molecular weight of PMMA used in this work is 950 000 Da compared to ~7000 Da of SU-8.[18] It is certainly possible that other combinations of time and temperature would produce the same results, e.g., lower temperature and longer time. In the case of SU-8, after initial heating at 55 °C to produce sloped sidewalls, the patterns were cured under UV exposure (450 mJ/cm^2) and underwent a postexposure bake on a hotplate at 95 °C for 1 min. Cross-linking the SU-8 under these conditions does not alter the profile shape further. Different polymers will require different conditions to produce the desired sidewall profile, as evidenced in the case of PMMA and SU-8 in Figs. 2(a) and 2(b). Such tunability is desirable as certain applications may have low temperature requirements. In the case of photolithography patterns, the dose is controlled such that after photolithography and development, the pattern profile is sloped, similar to Fig. 1(b). For S1813, underexposure at a dose of 50 mJ/cm^2 produces sloped side-

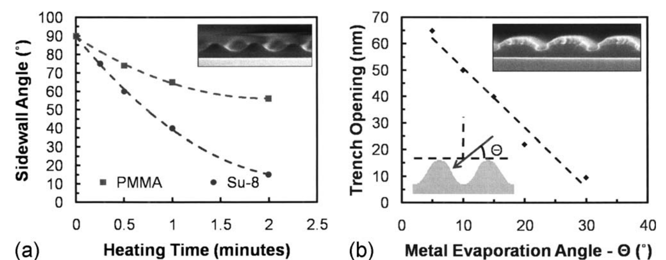

FIG. 3. (a) Slope angle of nanoimprinted grating sidewalls as a function of heating time for both PMMA and SU-8; inset in the top right shows a cross sectional SEM image of a sloped SU-8 grating. (b) Trench opening size as a function of metal evaporation angle for a typical sloped nanoimprinted grating; schematic inset in the bottom left illustrates the angle of metal evaporation (Θ) while the image inset in the top right shows a cross sectional SEM image of metal coating on the sloped grating.

walls, as shown in Fig. 2(c). These processes to control patterned polymer shape, both with imprinted (SU-8 and PMMA) and photolithographically defined (S1813) gratings, have shown the polymer shape profile to be well controlled at low temperatures (as low as 55–85 °C for SU-8), which is desirable for a wide variety of materials, including plastic substrates.

After a sloped sidewall profile is produced, the next step is selective metal coating by shadow or oblique angle metal evaporation. The metal is selectively coated onto both sides of sloped polymer grating sidewalls to produce small openings in between the metal, the size of which is determined by the angle at which the metal is coated. The approximate size of openings can be predicted by trigonometry, with higher angles producing smaller openings. It is possible that shadow evaporation over large areas could introduce global critical dimension variations. The uniformity in size of openings across large areas depends not only on the sample size but also on the distance from metal source and configuration of the metal source. For especially large samples, it may be beneficial to use slightly deeper sloped grating patterns with steeper slope so that higher angle shadow evaporation can be used to create small gaps. Figure 3(b) shows the trench opening width with respect to the angle of metal evaporation for a typical nanoimprinted grating with sloped sidewalls, indicating a linear relationship, which affords a high degree of control in the final trench dimension (down to 8–10 nm). Electron-beam deposition was used to evaporate the metal, as a directional physical deposition method is required for controlled shadowing. The quality of the metal coating can play a role in final LER after pattern transfer. For uniform metal coating with minimal roughness, a low chamber pressure ($<10^{-6}$ Torr) and a low deposition rate (~ 0.5 Å/s) were used. Cr was used as the etching mask, as it is easily evaporated by e-beam deposition and provides sufficient selectivity to SiO_2 in fluorine plasma.

After 15–30 nm Cr evaporation, the samples underwent plasma etching in inductively coupled plasma (ICP) for minimal angular spread of the incoming ions to produce straight sidewalls. First, the samples were etched in oxygen plasma (300 W ICP power, 100 W bias power, 5 mTorr, 25 °C chuck temperature, ~ 10 s) to remove the polymer residue exposed in between the metal openings. After the residue was etched, the pattern was transferred to the oxide layer by etching in a mixture of C_4F_8, CHF_3, and Ar with conditions that have been optimized to produce straight sidewalls (2000 W ICP, 500 W bias, 5 mTorr, 10 °C, ~ 10 s). At this point, the pattern can be further etched into the silicon, if desired. Figures 4(a)–4(c) show cross sectional scanning electron microscopy (SEM) images of dimension reduced nanotrenches transferred to the oxide layer. The Cr etch rate in these plasma etching steps is sufficiently low, as evidenced by the residual Cr that is clearly visible even after pattern transfer to underlying oxide in Figs. 4(b) and 4(c). Trench dimensions of less than 10 nm have been produced using this method, with reasonable uniformity, reduced from the original 100 nm line and space gratings. This demonstrates a ten times well-controlled size reduction. Figure 4(d) shows a cross sectional SEM image of dimension reduced trenches in S1813; the trench dimension has been reduced to ~ 200 nm from the original ~ 1 μm. With higher angle metal evaporation, it is possible to scale the ~ 1 μm gratings to well below 100 nm. The final transferred trench dimension can be tuned not only by the angle of metal evaporation but also by the slope of the grating sidewalls, providing two degrees of control. With such control, it is possible to produce uniform dimension reduced nanogratings over large areas with precision, as shown in Figs. 4 and 5. As expected, the lines are smooth and uniform and the cross sections exhibit excellent profiles. Any defects or nonuniformities in the dimension reduced lines are likely a result of original patterning, as seen in Fig. 6, which shows several defects in a small area of the original imprinted SU-8 patterns. Variations in smoothness and height of original imprinted lines, both along a line and among adjacent lines, will result in variations in final grating slope and height, which, in turn, will directly affect shadowed Cr coating. Therefore, nonuniformity in the original patterns would lead to LER in final dimension reduced patterns. Small scale LER (local roughness) largely depends on the quality of metal coating and subsequent etching during pattern transfer. Therefore, it is necessary to optimize metal deposition and etching conditions if smaller LER is required.

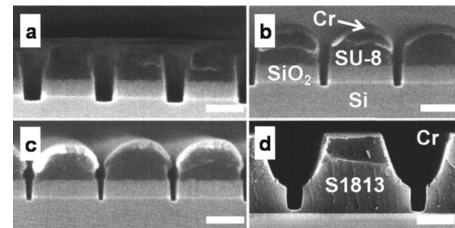

FIG. 4. Cross sectional SEM images of dimension reduced gratings with widths of (a) ~ 50 nm, (b) ~ 20 nm, (c) 8–10 nm, and (d) ~ 200 nm. (a), (b), and (c) are dimension reduced nanoimprinted gratings [scale bars are 100 nm; materials in (a), (b), and (c) are the same] while (d) is a dimension reduced microscale grating originally defined by photolithography (scale bar is 650 nm).

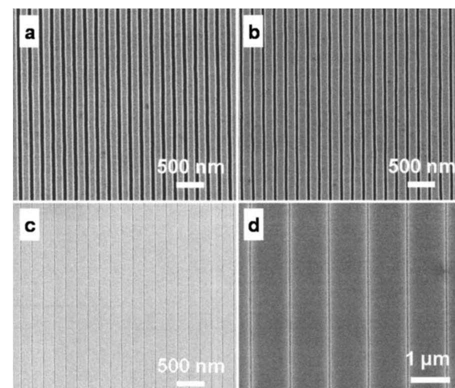

FIG. 5. Top view SEM images of dimension reduced gratings with widths of (a) ~ 75 nm, (b) ~ 50 nm, (c) 8–10 nm, and (d) ~ 200 nm. (a), (b), and (c) are dimension reduced nanoimprinted gratings while (d) is a dimension reduced microscale grating originally defined by photolithography.

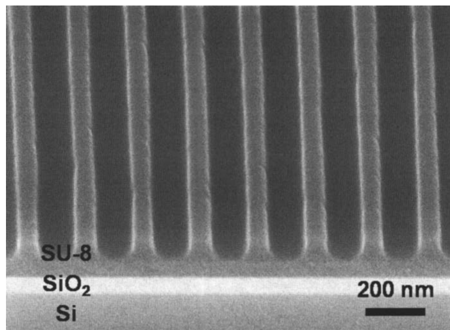

FIG. 6. Tilted (45°) SEM image of original imprinted SU-8 patterns.

One of the limitations of this method is the inability to reduce the pitch of the original grating, which, in our case, was defined by a mold fabricated with interference lithography[19] (in the case of nanoimprinted gratings) or by the dimensions of patterns on the mask (in the case of photolithographically defined gratings). As defining ultrafine gratings ($\sim$10 nm) is challenging and/or expensive for photolithography and interference lithography, combining our dimension reduction method with these two techniques may provide a unique means to define ultrasmall nanograting patterns over large areas.

III. CONCLUSION

In this work, we have developed a simple dimension reduction process to make nanoscale gratings down to sub-10-nm width over large areas. Dimension reduction is achieved by controlling the shape and slope of patterned polymer grating sidewalls, followed by oblique angle evaporation and plasma etching to define openings with up to ten times reduction in size. As we have shown, this process is scalable to both microscale and nanoscale gratings, relaxing the requirements for high resolution lithography. Low temperature processing allows the use of a wide variety of materials. The controllability inherent to this process affords a high degree of precision in dimension and uniformity of size reduced nanogratings.

ACKNOWLEDGMENTS

This research was supported by the Air Force Office of Scientific Research through the SPRING program (Grant No. FA9550-06-1-0403) and KETI through the international collaboration program of COSAR, “Next generation semiconductor technology, equipments and materials.”

[1] L. J. Guo, X. Cheng, and C. F. Chou, Nano Lett. **4**, 69 (2004).
[2] D. L. Brundrett, T. K. Gaylord, and E. N. Glytsis, Appl. Opt. **37**, 2534 (1998).
[3] E. Stern *et al.*, Nature (London) **445**, 519 (2007).
[4] M. S. Kim, J. S. Kim, J. C. Cho, M. Shtein, L. J. Guo, and J. Kim, Appl. Phys. Lett. **90**, 123113 (2007).
[5] A. S. Crouch, D. Miller, K. J. Luebke, and W. Hu, Biomaterials **30**, 1560 (2009).
[6] B. D. Gates, Q. B. Xu, M. Stewart, D. Ryan, C. G. Willson, and G. M. Whitesides, Chem. Rev. (Washington, D.C.) **105**, 1171 (2005).
[7] Y. Chen and A. Pepin, Electrophoresis **22**, 187 (2001).
[8] S. Y. Chou, P. R. Krauss, and P. J. Renstrom, J. Vac. Sci. Technol. B **14**, 4129 (1996).
[9] Y. Zhao, E. Berenschot, M. de Boer, H. Jansen, N. Tas, J. Huskens, and M. Elwenspoek, J. Micromech. Microeng. **18**, 064013 (2008).
[10] Y. K. Choi, J. Zhu, J. Grunes, J. Bokor, and G. A. Somorjai, J. Phys. Chem. B **107**, 3340 (2003).
[11] Q. F. Xia, K. J. Morton, R. H. Austin, and S. Y. Chou, Nano Lett. **8**, 3830 (2008).
[12] X. M. Yan, S. Kwon, A. M. Contreras, J. Bokor, and G. A. Somorjai, Nano Lett. **5**, 745 (2005).
[13] S. Y. Chou and Q. F. Xia, Nat. Nanotechnol. **3**, 295 (2008).
[14] Y. Wang, X. G. Liang, Y. X. Liang, and S. Y. Chou, Nano Lett. **8**, 1986 (2008).
[15] X. Yang, H. Gentile, A. Eckert, and S. R. Brankovic, J. Vac. Sci. Technol. B **22**, 3339 (2004).
[16] D. L. Klein, R. Roth, A. K. L. Lim, A. P. Alivisatos, and P. L. McEuen, Nature (London) **389**, 699 (1997).
[17] G. Philipp, T. Weimann, P. Hinze, M. Burghard, and J. Weis, Microelectron. Eng. **46**, 157 (1999).
[18] A. L. Bogdanov, Proc. SPIE **3999**, 1225 (2000).
[19] T. A. Savas, M. L. Schattenburg, J. M. Carter, and H. I. Smith, J. Vac. Sci. Technol. B **14**, 4167 (1996).